Chemical Geology 384 (2014) 16–26

Contents lists available at ScienceDirect

Chemical Geology

journal homepage: www.elsevier.com/locate/chemgeo

Solid-phase phosphorus speciation in Saharan Bodélé Depression dusts and source sediments

Karen A. Hudson-Edwards [a,*], Charlie S. Bristow [a], Giannantonio Cibin [b], Gary Mason [a], Caroline L. Peacock [c]

[a] Department of Earth and Planetary Sciences, Birkbeck, University of London, Malet St., London WC1E 7HX, UK
[b] Diamond Light Source, Harwell Science and Innovation Campus, Didcot, Oxfordshire OX11 0DE, UK
[c] School of Earth and Environment, University of Leeds, Leeds LS2 9JT, UK

ARTICLE INFO

Article history:
Received 20 February 2014
Received in revised form 17 June 2014
Accepted 19 June 2014
Available online 29 June 2014

Editor: J. Fein

Keywords:
Bodélé Depression
Sahara
Dust
Phosphorus
Fish
Apatite

ABSTRACT

Phosphorus (P) is one of the most important limiting nutrients for the growth of oceanic phytoplankton and terrestrial ecosystems, which in turn contributes to CO_2 sequestration. The solid-phase speciation of P will influence its solubility and hence its availability to such ecosystems. This study reports on the results of X-ray diffraction, electron microprobe chemical analysis and X-ray mapping, chemical extractions and X-ray absorption near-edge spectroscopy analysis carried out to determine the solid-phase speciation of P in dusts and their source sediments from the Saharan Bodélé Depression, the world's greatest single source of dust. Chemical extraction data suggest that the Bodélé dusts contain 28 to 60% (mean 49%) P sorbed to, or co-precipitated with, Fe (hydr)oxides, <10% organic P, 21–50% (mean 32%) detrital apatite P, and 10–22% (mean 15%) authigenic–biogenic apatite P. This is confirmed by the other analyses, which also suggest that the authigenic–biogenic apatite P is likely fish bone and scale, and that this might form a larger proportion of the apatite pool (33 +/− 22%) than given by the extraction data. This is the first-ever report of fish material in aeolian dust, and it is significant because P derived from fish bone and scale is relatively soluble and is often used as a soil fertilizer. Therefore, the fish-P will likely be the most readily consumed form of Bodélé P during soil weathering and atmospheric processing, but given time and acid dissolution, the detrital apatite, Fe-P and organic-P will also be made available. The Bodélé dust input of P to global ecosystems will only have a limited life, however, because its major source materials, diatomite in the Bodélé Depression, undergo persistent deflation and have a finite thickness.

1. Introduction

Phosphorus (P) is one of the most important limiting nutrients for the growth of oceanic phytoplankton and terrestrial ecosystems (Swap et al., 1992; Ammerman et al., 2003); processes that lead to N_2 fixation and CO_2 sequestration (Swap et al., 1992; Okin et al., 2004; Mahowald et al., 2008). In these ecosystems, aqueous P is derived by the dissolution of P-bearing solids (Filippelli, 2008) that include aeolian dusts (Swap et al., 1992; Okin et al., 2004), which are in turn considered to be the dominant sources of P in the atmosphere (Pett-Ridge, 2009). In dusts, P mainly occurs in minerals of the apatite family and as sorbed species to (Fe hydr)oxides (Eijsink et al., 2000; Singer et al., 2004), but can also occur as organic-P (Filippelli, 2008) and as anthropogenically-produced particles (e.g., coal combustion, biomass burning; Winter et al., 2002; Dolislager et al., 2012). The solid-phase speciation of P will influence its solubility (Fulmer et al., 2002; Anderson et al., 2010; Nenes et al., 2011).

Saharan dusts are thought to provide significant amounts of P to the eastern tropical Atlantic (Washington et al., 2006; Schepanski et al., 2009), to the Amazon basin (Swap et al., 1992; Koren et al., 2006; Bristow et al., 2010), whose terrestrial productivity is P-limited (Sanchez et al., 1982; Okin et al., 2004), and to other areas throughout the world (e.g., the Southern Ocean). The Saharan Bodélé Depression, representing part of palaeo-lake Mega-Chad in the southern Sahara in Chad, is the world's greatest single source of dust (Washington et al., 2003) (Fig. 1). Dusts from the Bodélé traverse the African Savannah, the Gulf of Guinea, equatorial Atlantic and the Amazon, and also cover the Pacific and Southern Oceans. Bristow et al. (2010) estimated that 33,000–94,000 t of P and 8500–29,000 t of P are deposited annually in the equatorial Atlantic and Amazon, respectively. Palaeo-lake Mega-Chad, with an area of at least 350,000 km^2 (10,000 × 6000 km) was formerly the largest lake in Africa around 6000 years ago (Schuster et al., 2005; Drake et al., 2006). Since then, a change in climate has caused the lake to dry out and the Bodélé now comprises an east–west elongated basin c. 500 km long, 150 km wide and 160 m deep covering an area of 133,352 km^2 (Bristow et al., 2009). Apart from Lake Chad in the southern basin (Fig. 1), the lake bed is dry. At the centre of the Bodélé Depression is 24,049 km^2 of authigenic diatomite-rich sediments of

* Corresponding author.
E-mail address: k.hudson-edwards@bbk.ac.uk (K.A. Hudson-Edwards).

http://dx.doi.org/10.1016/j.chemgeo.2014.06.014

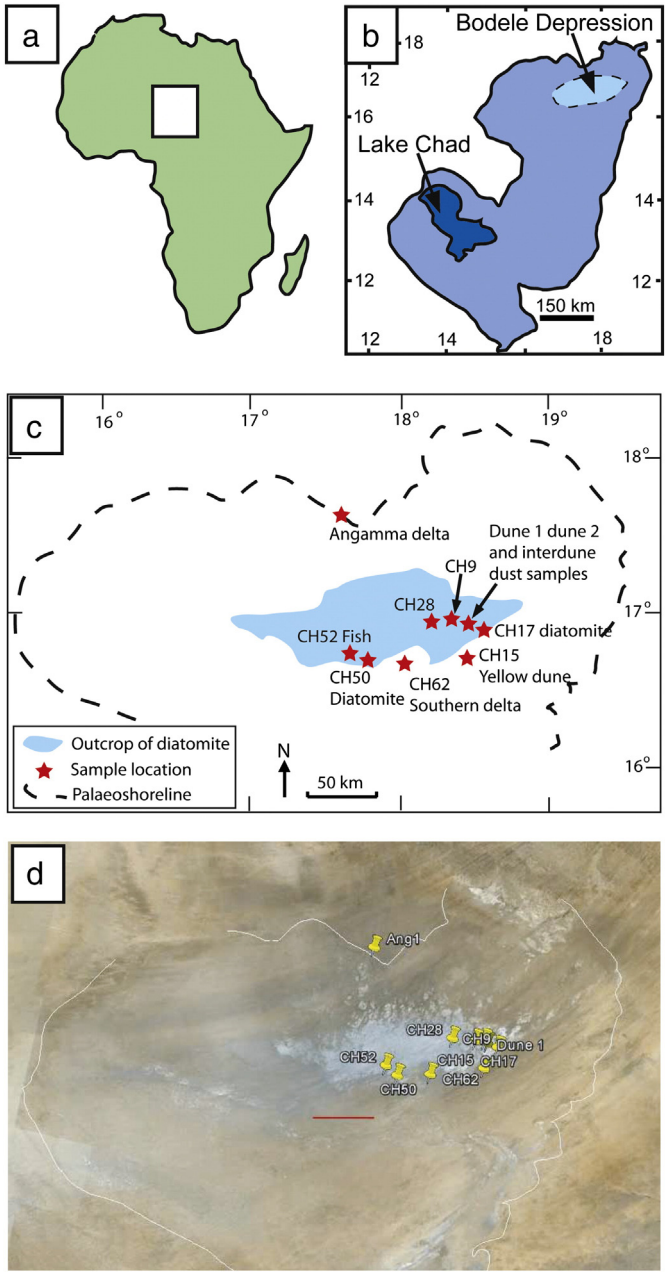

Fig. 1. Location of the Bodélé Depression and samples used in this study. (a) Map of Africa with inset box (b) Showing location and extent of palaeolake Megachad, Lake Chad, and the Bodélé Depression, (c) Sample location map, showing diatomite outcrop and extent of the palaeo shoreline, (d) Google Earth image of area in (c). Red line is 50 km scale bar as shown in (c). (For interpretation of the references to color in this figure legend, the reader is referred to the web version of this article.)

Holocene age (hereafter referred to as diatomite), which are clearly visible on satellite images due to their high albedo (Fig. 1). The diatomite consists of mostly hollow diatom frustules of biogenic silica that have a very low bulk density (c. 0.8 g cm^{-2}), are cemented by authigenic calcite, Mg-calcite, aragonite and gypsum, and are fragile and easily broken (Bristow et al., 2009, 2010). At least 4 m of the diatomite has been eroded over the past 1000 years due to saltation bombardment and aeolian erosion by strong surface winds from the Bodélé Low Level Jet (LLJ) (Washington and Todd, 2005; Washington et al., 2006; Bristow et al., 2009). The eroded Bodélé diatomite is the primary source of dust from the region (Bristow et al., 2009). Surrounding and underlying these sediments are lacustrine and fluvio-deltaic sediments from rivers that used to flow into palaeo-lake Mega-Chad, as well as aeolian sand derived from the Bodélé and Libya; these are also considered to be potential sources of dust (and are therefore referred to herein as 'other source sediments'), though to a lesser extent than the diatomite (Bristow et al., 2009).

Knowledge of the solid-phase speciation of P in Bodélé dusts will help to improve estimates of P inputs and their relative solubilities into areas where the dust is transported and deposited, such as the Amazon and tropical Atlantic. To this end, this study reports on chemical, mineralogical and spectroscopic analyses of Bodélé dusts and their source sediments, to determine the solid-phase speciation of P in these materials.

2. Methods and materials

2.1. Sample collection

Bodélé dust samples, and sediment samples that represent common sediments and the most likely dust sources within the Bodélé Depression, were collected in 2005 as part of the Bodélé Dust Experiment (BoDEX; Washington et al., 2006). The storm that generated the dust samples is described as 'modest' when compared with satellite observations of Bodélé dust plumes (Washington et al., 2006). Diatomite and diatomite surface sediments were collected from outcrops and on the surface of the diatomite, and the 'other source sediments' were collected from outcrops of dunes and of sediments that are eroded and deposited in the Bodélé Depression. The Grey Dune sediment sample CH9 (Fig. 2a) is largely composed of sand to granule sized pieces of diatomite reworked and eroded from the lakebed, together with a minor component of quartz sand grains eroded from the underlying fluvial sediments as well as quartz grains blown in from upwind. XRD analysis of a neighbouring diatomite dune (sample CH8, 650 m to the SE) indicates the presence of kaolinite, quartz, muscovite and mixed layer clays that are interpreted as detrital minerals derived from weathering and erosion in the hinterland and blown or washed into the lake basin. The Yellow Dune sand CH15 (Fig. 2b) is composed of fine to medium grained quartz sand. These Yellow Dune sands can be distinguished on satellite images and traced upwind towards the northeast to the Great Sand Sea in southern Libya and western Egypt.

Sample CH17 is from the base of an outcrop of white well-bedded diatomite overlying Yellow Dune sand close to Chicha (Fig. 2c). It contains aragonite and calcite, which are authigenic cements within the diatomite, and quartz, kaolinite and albite, which are detrital, either being washed or blown into the lake. XRD analysis of an overlying diatomite sample CH19 indicates the presence of kaolinite, muscovite and quartz that are interpreted to have been washed or blown into the lake and accumulated within the diatomite. Sample CH50 is also from an outcrop of diatomite that overlies dune sands (Fig. 2f), but it is located around 85 km to the WSW (Fig. 1). Viewed under SEM the sample contains abundant hollow tubes that are the frustules of freshwater diatom *Aulacoseira* spp., and aragonite, calcite, gypsum, kaolinite, and quartz are also present (Bristow et al., 2009). The kaolinite and quartz are interpreted to have been blown or washed into the lake, while the aragonite, calcite and gypsum are interpreted to have precipitated within the sediments during early diagenesis as or soon after the lake waters evaporated. Sample CH28 is a surface diatomite sample. It contains calcite, which is likely authigenic, and quartz and kaolinite, which are most likely to be detrital. CH28 also contains fish bone and scale materials, which were subject to separate XRD analysis (see below).

Sample CH39 is a very fine- to fine-grained, silty sand with ostracod valves (Fig. 2e). It was collected from the Angamma Delta, a wave-influenced delta fed by a braided river that flowed into the Bodélé Depression from the Tibesti Mountains in the north. XRD analysis indicates the presence of kaolinite, muscovite, albite and quartz as well as mixed layer clays. The presence of albite feldspar and mixed layer clays within the Angamma Delta sediments distinguishes them from the other Bodélé sediments and is attributed to the presence of volcanic rocks in the hinterland, in particular the volcano Emi Kousi, which is around

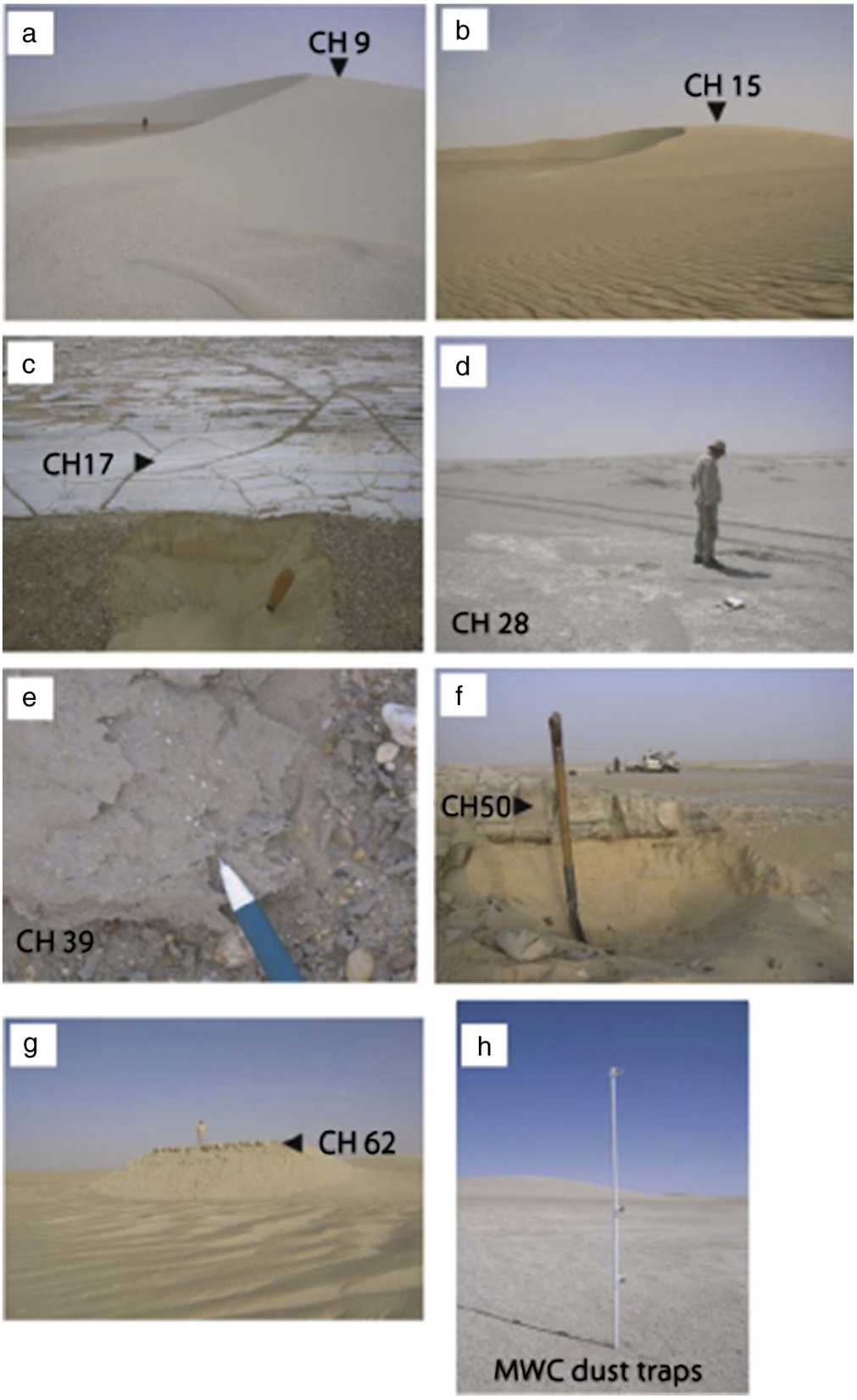

Fig. 2. Field photographs of sample locations. (a) CH9 grey diatomite dune with person for scale; (b) CH15 Yellow Dune, which is similar in size to that in (a); (c) CH17 diatomite overlying yellow dune sand near Chicha, with trowel handle for scale; (d) CH28 surface sediments composed of broken pieces of diatomite, with person for scale; (e) CH39 silty sand with ostracods from Angamma Delta, pen for scale; (f) CH50 diatomite overlying dune sand, with spade for scale; (g) CH62 clay overlying sand from Southern Delta, with person for scale; (h) example of mast with dust traps at 0.75 m, 1.4 m and 2.4 m above ground.

Fig. 3. Photograph of two grey dunes. These are migrating across a dark interdune surface with large barchanoid dunes on a pale diatomite interdune surface in the background. The darker surface is attributed to iron stained grains that cap fluvial distributary channel deposits that locally underlie the diatomite, and from which a cover of diatomite has been removed by deflation (Bristow et al., 2009, Chappell et al. 2008).

250 km NNE from the delta. Sample CH62 is taken from a 30 cm layer of clay that caps an outcrop of pale pink sand on the southern side of the Bodélé Depression close to the Bahr el Ghazal (South Delta sample, Fig. 2g). The Bahr el Ghazal is an overflow channel that links the Bodélé Depression in the north with Lake Chad in the south. When water levels in Lake Chad reach an elevation of around 290 m, approximately 10 m above the modern lake level, the lake waters can spill over a sill and flow north into the Bodélé via the Bahr el Ghazal. XRD analysis of the clays shows that they are kaolinite, which is most likely derived from a deeply weathered hinterland to the south and southeast, most likely equivalent to the catchment of the modern Chari River, which is the pre-eminent influent for Lake Chad.

Dust samples were taken during a three-day dust storm from 10th to 12th March 2005 from three separate dunes as well as from the interdunes. The samples were collected using MWAC (Modified Wilson and Cooke) samplers (Fig. 2h), which allowed dust in suspension to enter a container via an inlet tube and settle allowing the air to return to the atmosphere via an outlet tube. The drop in pressure within the container allows the air to slow and the dust to fall from suspension. Samples were only taken from the 'mid' traps on the apparatus at a height of 1.4 m, as lower dust traps were not used to avoid load from saltation in an attempt to obtain suspended load rather than samples emitted from particle collision on the desert floor, or those too heavy to be carried into the atmosphere, and the upper traps rarely captured sufficient sediments for chemical analysis. Three of the dust samples were collected from masts erected on grey diatomite barchan dunes (21-mid, 27-mid and 32-mid; e.g., Fig. 3), of these 21-mid and 27-mid were on the same dune (Dune 1) with 21-mid on the upwind side of the dune and 27-mid on the northern horn of the barchan. Sample 32-mid was 128 m upwind of the crest of Dune 2 (Chappell et al., 2008). Seven of the samples were collected from masts erected on the interdune surface (40-mid, 57-mid, 59-mid, 60-mid, 66-mid, 67-mid, 73-mid). Of these, four samples (40-mid, 66-mid, 67-mid, and 73-mid) were erected on diatomite surfaces that were covered in chips of broken diatomite, as well as reworked, rounded clasts of diatomite. Three of the samples (57-mid, 59-mid, 60-mid, and 60-mid) were

Table 1
Description of Bodélé samples.

Sample type	Sample number	Source	Latitude	Longitude	Total P (ppm)
Sediment	CH15	Yellow Dune	16°43′32.4″ N	18°26′17.3″ E	40
Sediment	CH39	Angamma Delta	17°56′54.0″ N	17°36′11.2″ E	970
Sediment	CH62	South Delta	16°41′03.2″ N	18°01′42.0″ E	420
Sediment	CH28	Surface diatomite sediment	16°56′54.0″ N	18°11′57.9″ E	590
Rock	CH17	Diatomite	16°52′48.5″ N	18°32′38.2″ E	610
Rock	CH50	Diatomite	16°40′35.8″ N	18°32′38.2″ E	600
Sediment	CH9	Grey Dune	16°55′47.7″ N	18°22′30.7″ E	580
Dust	21-mid	Dune 1	16°56′11.8″ N	18°26′48.7″ E	600
Dust	27-mid	Dune 1	16°56′03.4″ N	18°26′23.7″ E	930
Dust	32-mid	Dune 2	16°54′50.6″ N	18°27′56.6″ E	780
Dust	40-mid	Interdune	16°53′30.0″ N	18°28′36.8″ E	660
Dust	57-mid	Interdune	16°55′56.3″ N	18°26′14.3″ E	900
Dust	59-mid	Interdune	16°55′43.3″ N	18°25′56.7″ E	690
Dust	60-mid	Interdune	16°55′36.3″ N	18°25′47.3″ E	680
Dust	66-mid	Interdune	16°54′47.0″ N	18°27′25.8″ E	600
Dust	67-mid	Interdune	16°54′41.9″ N	18°27′25.9″ E	630
Dust	73-mid	Interdune	16°53′17.2″ N	18°28′19.9″ E	590

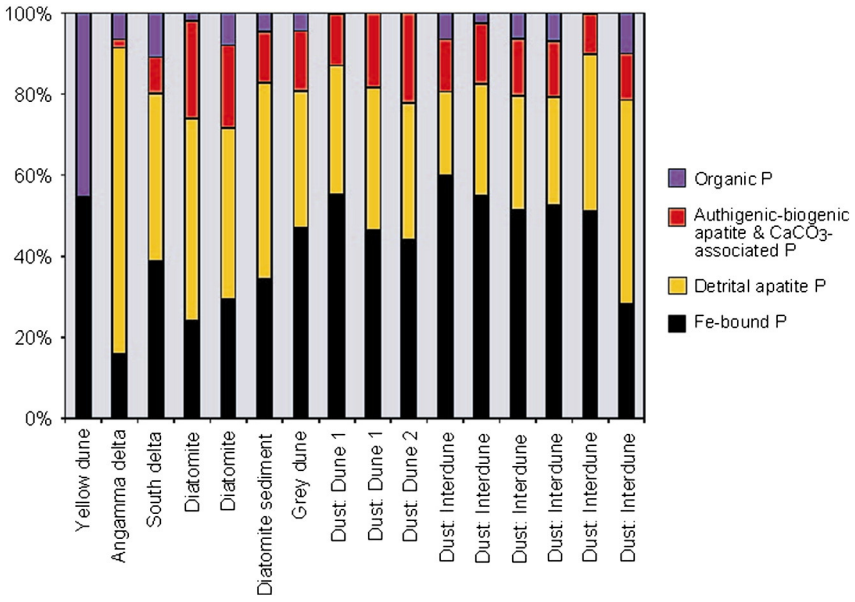

Fig. 4. Chemical extraction data for Bodélé diatomite, other source sediment and dust samples. All samples except the Yellow Dune contain Fe-bound P (extracted with a citrate/dithionite/bicarbonate solution), detrital apatite P (extracted with 1 N HCl without ashing), authigenic–biogenic apatite and $CaCO_3$-associated P (extracted with acetic acid/sodium acetate) and organic P (calculated as the difference between total P and detrital P). Fish bone, teeth and scales are normally extracted as authigenic–biogenic apatite and $CaCO_3$-associated P. The data suggest that the dusts contain significant amounts of Fe-bound P, detrital apatite P and authigenic–biogenic apatite and $CaCO_3$-associated P (i.e., fish P).

erected on a darker surface interpreted as exhumed fluvial distributary channels (Bristow et al., 2009), although the surface on which the masts were placed downwind from the north horn of Dune 1 was covered by granule ripples largely composed of reworked diatomite of up to 1 cm diameter (Chappell et al., 2008). The average D50 of these dust samples is 123.3 ± 7.6 μm (calculated from data in O'Donoghue, 2011). Therefore, these Bodélé dusts have considerably larger sizes than average atmospheric aerosols, which tend to have diameters of <10 μm (Kohfeld and Tegen, 2007). Such Bodélé dusts will likely display higher P concentrations than reported in this study if they are reduced in size during atmospheric transport, as, generally, geochemical concentration is inversely proportional to grain size (Förstner and Wittman, 1979).

Ten of the dust samples collected from the mid traps were selected for analysis by sequential extraction (Table 1); these had been previously analysed for total P by Bristow et al. (2010). Other source sediments were collected using a stainless steel trowel and stored in sealed polythene sample bags. Loose surface samples were scooped from the surface and placed directly into a sample bag. Consolidated diatomite samples were excavated by hand using a spade to get a clean face and then broken before being sampled. Fish bones, scales and teeth were hand-picked from source sediment sample CH28 (a surface sediment sample composed of granule and sand sized pieces of diatomite with fine quartz sand; Fig. 2d) using a binocular microscope and plastic tweezers, for X-ray diffraction (XRD) and X-ray absorption near edge spectroscopy(XANES) analysis.

2.2. Chemical extractions and total P analysis

A five-step procedure was carried out to determine the operationally-defined chemical speciation of P in the dusts and source sediments. The procedure was based on, and modified from, those of Berner and Rao (1994), who analysed P speciation in wet sediments of the River Amazon and Amazon estuary, and Chen et al. (2006), who analysed P speciation in dry coastal aerosols. Four sub-samples were required for the five step procedure and 0.2 g of Bodélé dust or source sediment was used in each sample; this amount being dictated by the amounts available after previous geochemical analysis (Bristow et al., 2010). Steps one and two used one sub-sample to determine the loosely sorbed P and Fe-bound P using 20 ml CDB (sodium citrate/dithionite/bicarbonate pH 7.6) solution, followed sequentially by extraction of the authigenic–biogenic apatite and $CaCO_3$-bound P, using 20 ml of a buffered sodium acetate solution (pH 4.0). Step three extracted the total inorganic P using 20 ml of 1 M HCl on the second sub-sample with no ashing. Step four used the third sub-sample to measure total P by extraction with 20 ml of 1 M HCl after being ashed at 550 °C in an oven for 2 h. Total organic P was calculated as the difference between steps three and four (total P minus total inorganic P). Step 5 used the fifth subsample to measure water-soluble P by extraction with 20 ml of ultrapure 18 MΩ-cm deionized water (DIW). All samples were agitated on rollers for a minimum of 2 h (maximum 16 h overnight where necessary), then spun down on a centrifuge to gain the supernatants for analysis, which were drawn off individually into 10 ml vials and stored at room temperature. To determine detection limits and assess background concentrations of P procedural blanks were used at all steps in all sample sets. Reproducibility was assessed using duplicates, and accuracy was assessed by comparing total P concentrations obtained in step 4 to those obtained by digestion in HF-HNO_3 (Bristow et al., 2010), and both were considered acceptable. All solutions were then analysed by inductively coupled plasma optical emission spectrophotometry (ICP-OES, Ultima-JY). Total P concentrations in source sediment samples were also determined by ICP-OES analysis following the HF-HNO_3 digestion method described in Bristow et al. (2010).

2.3. X-ray diffraction

Fish scale and bone samples from CH28, and the WIL fluorapatite from the Liscombe deposits, Wilberforce, Ontario, Canada (Barbarand et al., 2003) were analysed by X-ray Powder Diffraction (XRD) analysis of air-dried, randomly oriented powder samples using a Bruker D8 Advance powder diffractometer and Cu-Kα radiation (λ = 1.5406 Å). Diffractograms were recorded at 25 °C, from 2°2θ to 82°2θ with 0.02° step-size and 310 s acquisition time per step. Bulk XRD analysis of the source rocks and sediments, and dusts, was carried out using a Philips PW1710 diffractometer and Cu-Kα radiation (λ = 1.5406 Å) with a PW 1730 generator, graphite monochromator and PC-APD software. Diffractograms were recorded at 25 °C, from 2°2θ to 70°2θ with a scan rate of 0.5°2θ per minute.

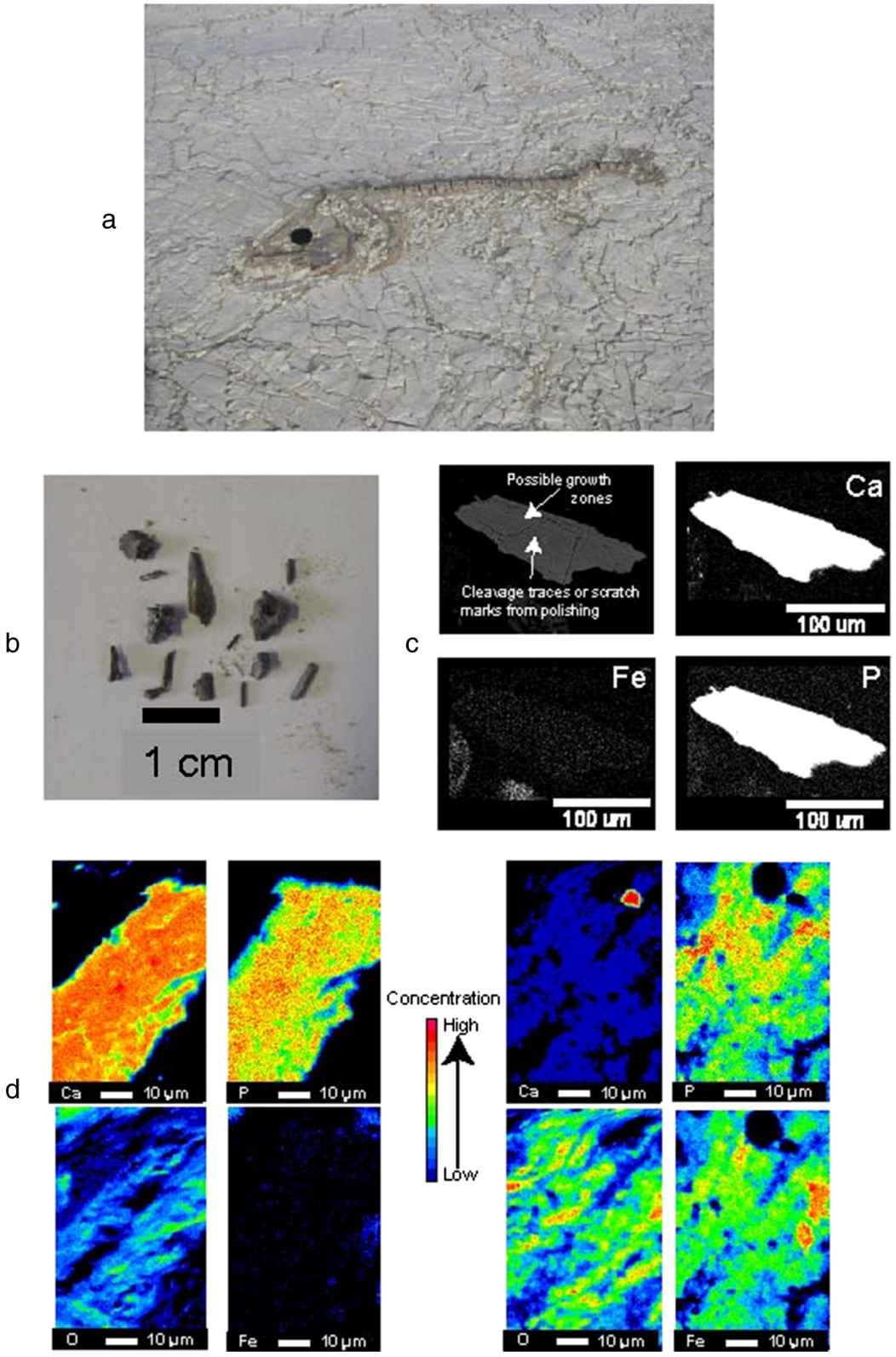

Fig. 5. Fish, calcium phosphate and Fe oxide associated phosphate materials in the Bodélé source sediment and dust samples. (a) Sub-fossil skeleton of a 1.15 m long Nile Perch preserved within diatomite on the floor of palaeolake Mega Chad within the Bodélé (locality CH52 shown in Fig. 1) (b) Fish scales, bones and teeth from diatomite sample CH28. (c) X-ray map of c. 200 μm long Ca–P (−O, not shown) fragment from Grey Dune sediment sample CH9 exhibiting possible growth zoning. The fragment contains no Fe, and has a molar Ca–P–O ratio typical of apatite. (d) X-ray map showing Ca–P–O grain from dust sample 21-mid, and Fe–P–O grain from dust sample 40-mid.

2.4. Electron microprobe analysis and X-ray mapping

Polished blocks of the resin-impregnated samples were subjected to electron microprobe micro-analysis (EPMA) with a Jeol JXA 8100 Superprobe equipped with wavelength dispersive spectrometers (WDS) and an Oxford Instrument Inca energy dispersive system (EDS). WDS X-ray mapping of the distribution of O, Si, Ca, Al, P and Fe was carried out using an accelerating voltage of 15 kV, current of

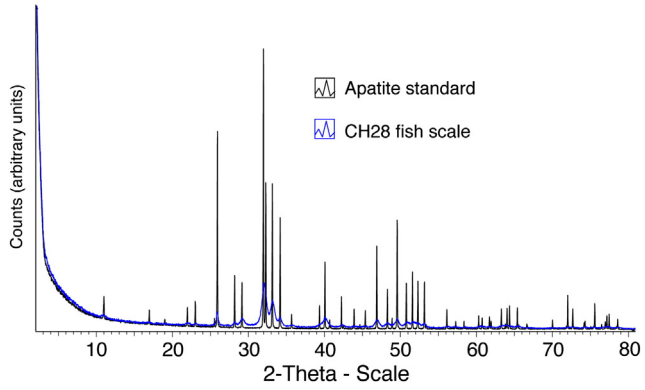

Fig. 6. XRD diffractogram of fish scale fluorapatite and apatite standard ICDD File 00-015-0876.

2.5 nA, electron beam diameter of 1 μm, and counting time of 20 s on peaks and 10 s on high and low backgrounds. The analyses were calibrated against standards of natural silicates, oxides and Specpure® metals with the data corrected using a ZAF programme. EDS mapping of homogeneous grains was also undertaken using an Oxford Instrument Inca system.

2.5. X-ray Absorption Near-Edge Structure (XANES) analysis

XANES analysis is a proven technique used to determine solid-phase P speciation on soils (Giguet-Covex et al., 2013). We conducted XANES analysis at the phosphorus *K*-edge (2149 eV) on station B18 at the Diamond Light Source Ltd. UK. Operating conditions for the storage ring were 3.0 GeV and 200 mA. The X-rays are collimated by a plane bent collimating mirror, and are then focused by a toroidal mirror after being monochromated by a Si (111) double-crystal monochromator. Data were collected at room temperature in the Soft X-ray experimental chamber with an unfocused beam, using a 4-element Vortex Silicon Drift fluorescence detector for the samples and Total Electron Yield in drain current mode for the standards. Powders of the Bodélé dusts and source sediments were analysed in fluorescence mode, and reference compounds Zn phosphate, vivianite, Al orthophosphate, WIL fluorapatite (Barbarand et al., 2003), fish scale and bone from source sediment sample CH28 (for authigenic–biogenic apatite) and synthetic PO_4-sorbed goethite, prepared according to the methods of Schwertmann and Cornell (1991) (for goethite) and Khare et al. (2005) (for PO_4 sorption, but using NaCl as an electrolyte background and NaH_2PO_4 instead of KCl and KH_2PO_4), were analysed in Total Electron Yield mode. The good energy resolution of the Vortex detector, in particular after optimization of the acquisition parameters, allowed discrimination of the P K line over a high background Si matrix signal from the dilute dust and source sediment samples. Between one and seven scans taking c. 1 to 1.25 h each were collected per sample.

XANES data reduction was performed using ATHENA (Ravel and Newville, 2005) and PySpline (Tenderholt et al., 2007). ATHENA was used to calibrate energy (eV) and to average multiple spectra from individual samples and standards. PySpline was used to perform background subtraction. For XANES data, the pre-edge was fit to a linear function and the post-edge background to one 2nd-order polynomial segment. XANES data were then normalized.

Linear combination modelling (LCM) of the background subtracted and normalized P XANES data, was performed in ATHENA. LCM of P XANES samples was done with a linear combination of the derivative μ(E) spectra from -20 eV to 30 eV either side of E_0, using WIL detrital fluorapatite, the fish scale poorly crystalline fluorapatite and the P-sorbed goethite as standards. The errors reported here for LCM fitting are those generated in ATHENA, i.e., 1-sigma error bars assuming the only source of noise is statistical noise (Ravel, 2009). Because XAS experiments are almost never dominated by statistical noise these errors are conservative; the error on fit components in two-component mixtures is estimated to be approximately ±10% of the stated value (Kim et al., 2000), due to, for example, differences in data reduction, and miss-match in central absorber coordination environment, between standards and samples.

3. Results and discussion

3.1. Characterisation of solid-phase P speciation in Bodélé dusts and source sediments

In sediments and dusts P can occur as detrital apatite, authigenic–biogenic apatite and $CaCO_3$-associated P, organic P, and be adsorbed to, or co-precipitated with, Fe oxides (Berner and Rao, 1994; Singer et al., 2004; Chen et al., 2006). Chemical extraction methods were used to determine whether some or all of these forms of P were present

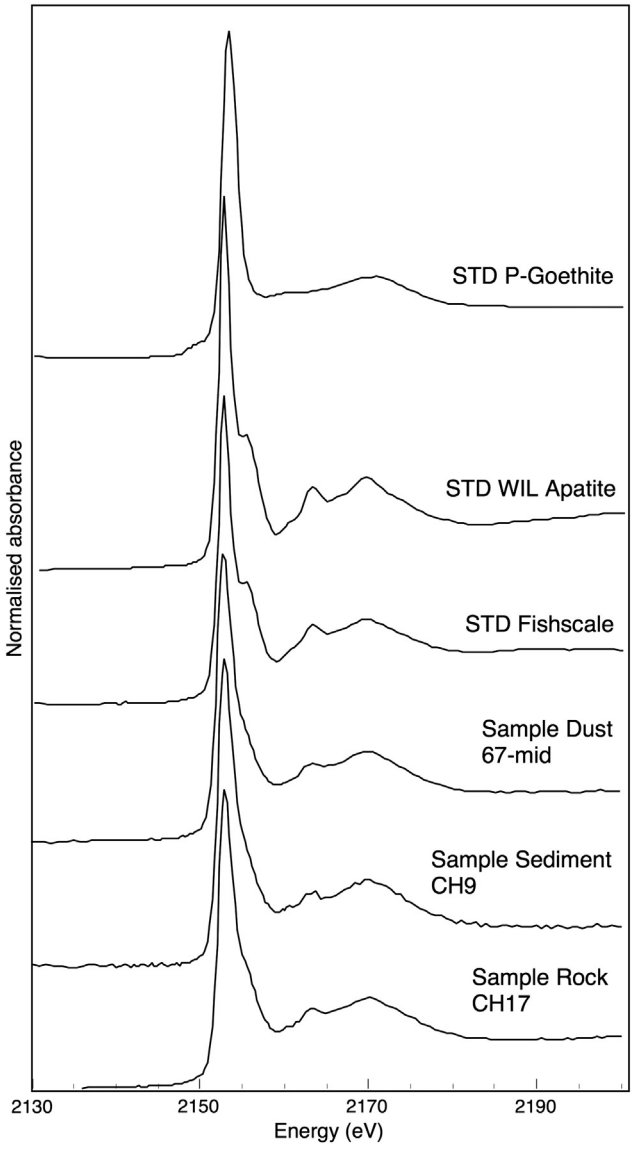

Fig. 7. Normalized P *K*-edge XANES data for detrital apatite, Bodélé fish scale and P-sorbed goethite standards, and Bodélé diatomite and dust samples. The profiles of the dust, diatomite and dune sediments are very similar to the poorly crystalline fluorapatite fish scale from the Bodélé diatomite in that they show dampened XANES features, suggesting that their apatite-P is at least partly fish-sourced. This is supported by linear combination modelling between the fish scale and P-sorbed goethite.

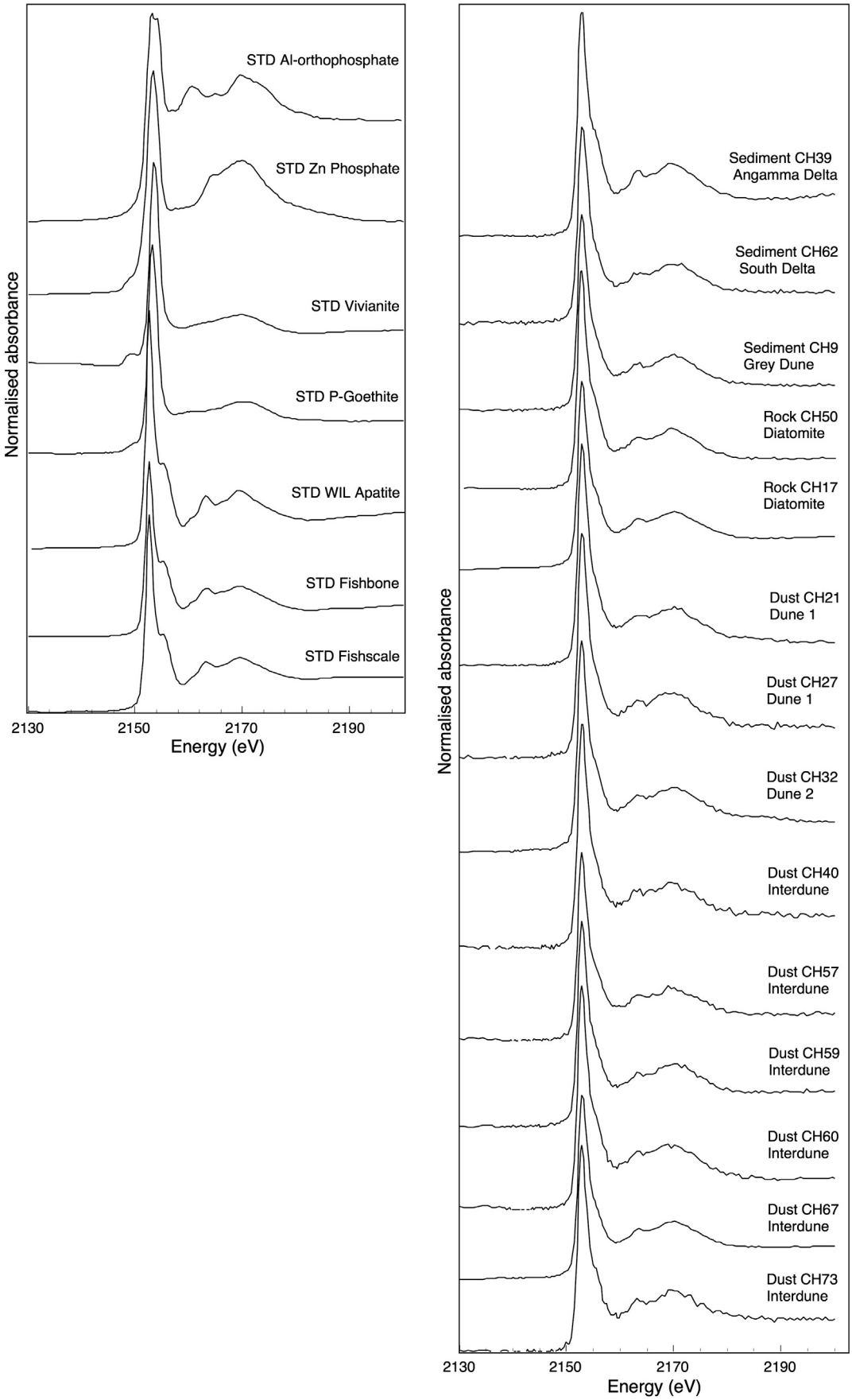

Fig. 8. Normalized P *K*-edge XANES data for standards and Bodélé source sediment and rock, and dust samples.

in Bodélé diatomite, other source sediments and dusts. Proportions of organic P are low (<10%) in all of the Bodélé samples except the Yellow Dune sediment, for which the large amount likely reflects the way in which organic P is determined (by subtraction from total inorganic P) and the very low total amount of P in this material (40 ppm). The chemical extraction data also suggest that 16 to 60% of the P in the Bodélé dusts, diatomite and other source sediments occurs as P sorbed to, or co-precipitated with, Fe (hydr)oxides (Fe-bound P; Fig. 4). Specifically, the dusts contain 28 to 60% Fe-bound P (mean 49%), more than the diatomite (24-29%) and Angamma Delta sediments (16%), but within the same range as the Grey Dune (47%), South Delta (39%) and Yellow Dune sediments (55%). The chemical extraction data for the dusts are validated by electron microprobe X-ray mapping, which shows that the dust P is associated with Fe–O-bearing phases (Fig. 5d).

Fossil Nile Perch skeletons occur in the Bodélé diatomite (Fig. 5a), as well as turtle and lungfish skeletons, and fish and vertebrate fossils have been found in sandstones that are considered to be sources of sediment to the Bodélé Depression (Schuster et al., 2009). Such fossil material can contain considerable amounts of P (Pasteris et al., 2008), and so the investigations also focused on whether the Bodélé dusts incorporated this important P source. The Bodélé diatomite contains fish scale, bone and teeth, and vertebrate bone fossils (Fig. 5b). X-ray diffraction (XRD) analysis shows that the fish scale and bone are composed of poorly crystalline fluorapatite (fluorine- (F-) bearing calcium phosphate; Fig. 6). In particular, Grey Dune sediments and Bodélé dusts contain up to 200 μm long, irregularly-shaped fragments of Ca–P–O material (Fig. 5c, d) that have Ca:P molar ratios and F contents (up to 2.6 wt.%) typical of fluorapatite. Many of these fragments exhibit irregular edge banding features that are interpreted as growth zones that occur in fish material (Fig. 5c; cf. Cooke and Jiménez, 2012). In addition, these Ca–P–O fragments are unlike most detrital apatites, which tend to be rounded, sub-rounded or partially euhedral (Mange and Maurer, 1991). The chemical extraction data provide evidence for the presence of both authigenic–biogenic apatite and $CaCO_3$-associated P (mean 15%, range 10–22%), and detrital apatite P (mean 32%, range 21–50%) in the Bodélé dusts (Fig. 4). The fish scale and bone would be extracted in the authigenic–biogenic apatite extraction, so this extraction indicates that there is an average of 15% fish P in the dusts. The amounts of fish-P are on the order of those in the diatomite and Grey Dune sediment (21–24% and 15%, respectively), and higher than those in the Yellow Dune, Angamma Delta and South Delta sediments (0%, 2% and 9%, respectively).

X-ray Absorption Near-Edge Structure (XANES) spectroscopy was used to provide further information about the types and relative proportions of P in the dusts and source materials. On visual comparison the dust profiles (exemplified in Fig. 7 with 67-mid) are very similar to the diatomite (exemplified in Fig. 7 with CH17) and Dune and Delta source sediments (CH9 Grey Dune), which are all very similar to the poorly crystalline fluorapatite fish material (fish scale) from the Bodélé diatomite, and the WIL fluorapatite (Barbarand et al., 2003) (Fig. 8). The position of the key spectral features, including a distinctive shoulder on the main absorption edge peak at 2155.6 eV, and higher energy secondary peaks at 2163.3 eV and 2170 eV, are consistent with XANES profiles of apatite-group minerals (Franke and Hormes, 1995; Ingall et al., 2011). These key features for the Bodélé fish material are dampened compared to the WIL fluorapatite, which indicates that the fish material is of poorer crystallinity (Ingall et al., 2011). This is consistent with the XRD analysis that shows the fish material is poorly crystalline fluorapatite (Fig. 6). The Bodélé dusts and source sediment profiles also show dampened features, pointing to their apatite-P being partly fish-sourced. The overall profiles of the dusts and source rocks and sediments also show some similarities to that of P-sorbed goethite (Fig. 7), but are dissimilar to those of the vivianite, Zn phosphate and Al-orthophosphate standards, which could be detrital P sources (Fig. 8). Given the strong evidence for the presence of authigenic–biogenic apatite P (Figs. 4 and 5b, c, d), detrital apatite P (Fig. 4) and P-sorbed Fe (hydr)oxides (Figs. 4 and 5d) in the Bodélé dusts, linear combination modelling (LCM) of dust sample 67-mid and diatomite sample CH17 with the fish scale (for authigenic–biogenic apatite P), the WIL apatite (for detrital apatite P) and the P-sorbed goethite standard, was carried out. The LCM indicates that the P in the dust samples is ~43% ± 10% fish material, ~3% ± 10% detrital apatite and ~54 ± 20% P-sorbed Fe (hydr)oxide (reduced Chi^2 = 0.00204), while the P in the diatomite is ~33 ± 20% fish material, ~26 ± 20% detrital apatite and ~41 ± 30% P-sorbed Fe (hydr)oxide (reduced Chi^2 = 0.0050). These results roughly match the chemical extraction results, in that for the dusts, nearly half is apatite-P (mean 15% fish/authigenic–biogenic and 30% detrital apatite = 45% apatite) and half is Fe–P (mean 49%). For the diatomite, ~68% is apatite-P (average 22% authigenic–biogenic and 46% detrital) and 27% is Fe-bound P. The LCM, however, indicates that a larger proportion of the apatite pool is fish apatite than detrital apatite, particularly for the dusts. It is possible that the LCM is overestimating the fish apatite. The LCM attempts to fit a dampened spectrum for the dust sample, and since the fish apatite standard displays such a spectrum, the LCM will drive towards this. However, if the Bodélé dusts contain a less crystalline detrital apatite than the WIL fluorapatite used in the LCM, then the LCM will drive towards this, thus better matching the chemical extraction data. Despite this, LCM was used in a two-component mixture to try and distinguish between fish apatite and detrital apatite. Best fits are judged using the reduced Chi^2 value, where the lowest value indicates the best statistical fit to the data. The best fits to the dust and diatomite samples are provided by linear combination of the fish scale and P-sorbed goethite (dust ~54 ± 10% fish scale with ~46 ± 10% P-sorbed goethite, reduced Chi^2 0.0589; diatomite ~58 ± 10% fish scale with ~42 ± 10% P-sorbed goethite, reduced Chi^2 0.00553; Table 2), suggesting again that a significant proportion of the apatite-P in the Bodélé samples is derived from fish.

Table 2
Linear combination modelling of dust and diatomite samples using P-sorbed goethite and WIL apatite or Bodélé fish scale.

Sample	Standard			Reduced Chi^2
	P-sorbed goethite	WIL apatite	Fish scale	
Dust 67-mid	0.453 ± 0.018	0.547 ± 0.018	–	0.00644
	0.463 ± 0.018	–	0.537 ± 0.018	0.00589
Diatomite CH17	0.406 ± 0.017	0.594 ± 0.017	–	0.00576
	0.418 ± 0.017	–	0.582 ± 0.017	0.00553

P-sorbed goethite, WIL apatite and fish scale are the fit weights generated for these standards in ATHENA, where P-goethite + WIL apatite or fish scale = 1. Errors given are (conservative) 1-sigma errors generated in ATHENA. Absolute reduced Chi^2 values are not accurate and are reported for relative comparisons between fits only.

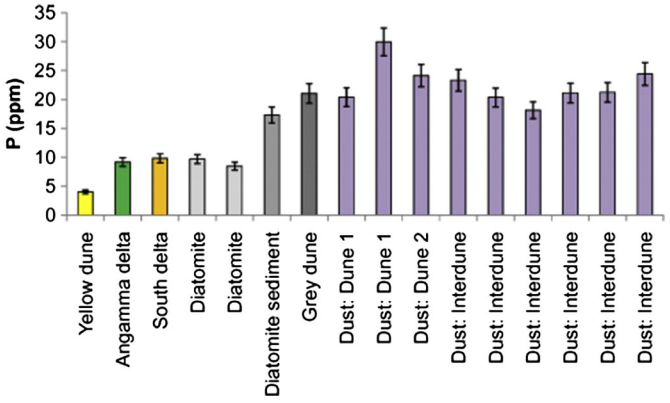

Fig. 9. De-ionised water extractions to estimate soluble fraction of phosphorus in Bodélé source sediments and rocks, and dusts.

3.2. Implications of Bodélé dust P speciation for terrestrial and ocean systems

Fish bone has been identified as a significant source of P in solids such as continental shelf and slope sediments of the Great Barrier Reef (Monbet et al., 2007), but ours is the first report in aeolian dust. The findings have important implications for the solubility of the solid forms of P in Bodélé dusts delivered to the Amazon, equatorial Atlantic and elsewhere in the world. Fish bones are a well-known soil fertilizer, and have been proposed as a cheap source of natural calcium phosphate (Boutinguiza et al., 2012). This is because they are formed of carbonate-substituted apatite (Cury et al., 2003) or apatite that is poorly crystalline (e.g., the Bodélé fish fluorapatite), both of which are more soluble than more crystalline detrital apatite (Smits et al., 2012). Therefore, the 10–15% (Fig. 4), and possibly up to 55% (LCM), authigenic–biogenic apatite/fish P in the Bodélé dusts likely provides significant amounts of relatively available P to soils and waters on which they are deposited. For example, Abouchami et al. (2013) presented isotopic evidence to show that Bodélé dusts reaching the Amazon were weathered rapidly upon arrival; in this case, the biogenic apatite/fish P would likely be the first to be weathered and made available as soil nutrients. It is acknowledged, however, that a larger proportion of the Bodélé dust P than just the fish P is likely to be available to Amazon and other worldwide soils supplied by the Bodélé dusts. It has been shown, for example, that mycorrhizal colonization can result in the extraction of P from insoluble phases (Smits et al., 2012), suggesting that over time, the detrital apatite-P, Fe–P and organic-P will also be weathered.

Because apatite-P and Fe-bound P phases are very insoluble in oceanic surface waters (which are alkaline and oxygenated; Atlas and Pytkowicz, 1977), the main source of bioavailable P from dusts is the water-soluble portion formed during acid leaching in the atmosphere (Nenes et al., 2011). To provide an estimate of the potential contribution of the Bodélé dusts to oceanic waters, chemical tests using circum-neutral pH deionized water as an extractant were conducted (Fig. 9). Between 28 and 30 ppm P is extracted from the dusts, representing 2 to 4% of their total P. If 33,000–94,000 t of P is deposited each year in the Atlantic from Bodélé dusts (Bristow et al., 2010) then this soluble fraction equates to 0.92–0.99 t P annually. Since atmospheric leaching tends to be acidic rather than circum-neutral (Nenes et al., 2011), this 0.92–0.99 t/a P is a minimum and the Bodélé dusts could supply considerably more leachable P to equatorial Atlantic phytoplankton. Nenes et al. (2011), for example, found that acid treatment of Saharan soil and dust samples released between 81 and 96% of the total P, from both apatite and Fe-bound P, and Anderson et al. (2010) estimated that 15–30% of total dust P was water-soluble. The global atmospheric P reservoir is estimated at 0.009×10^{12} mol (2.79×10^5 t; Richey, 1983; Jahnke, 1992; Mackenzie et al., 1993; Ruttenberg, 2007). The calculated 0.92–0.99 t/a water-soluble Bodélé P represents a very small proportion (3.30×10^{-4}% to 3.55×10^{-4}%) of this global reservoir.

On a geological time scale the Bodélé should be considered as a transient source of mineral dust and therefore, of the nutrient P. The Bodélé could not have been a dust source in the mid-Holocene, 6000 years ago, because the lake basin was flooded. Furthermore, the diatomite is a finite resource, which ongoing deflation will remove. The current thickness of the Bodélé sediments is unknown, and therefore it remains to be determined how long this important P source will last.

4. Conclusions

Dusts from the Bodélé Depression in Chad, the world's greatest single source of dust, contain P sorbed to, or co-precipitated with, Fe (hydr)oxides (28-60%), organic P (<10%), detrital apatite P (21–50%), and authigenic–biogenic apatite P (10–22%, but possibly up to 33 ± 22%) in the form of fish bone and scale. The fish P is likely the most soluble form of P in the Bodélé dusts, but the other forms will become available to global soils as they weather over time, and to oceanic waters as they undergo atmospheric processing. Our methods are similar to others analysing atmospheric P concentrations and P speciation (e.g., Chen et al., 2006), but oceanic-solubility estimates (using de-ionised water, and indicating that 2–4% of the total P is soluble) are different to other studies determining soluble aerosol P (e.g., Baker et al., 2006a, b, who used a Na-bicarbonate leach and found between 2.3 and 67% of the P was soluble). Therefore, significantly more than the 2–4% of the Bodélé dust P could be soluble to the oceans.

Acknowledgements

This research was funded by grants from the Gilchrist Educational Trust and the Royal Geographical Society (Gilchrist/RGS 2004-1) to C.S.B. We thank A. Beard for assistance with microprobe analysis, A. Osborn and G. Tarbuck for help with geochemical analysis, and A. Atkins for assistance with XRD data collection and analysis. We are grateful to M. Krom for commenting on an earlier version of the manuscript. We thank Diamond Light Source for access to beamline B18 (proposals NT1986 and sp7527) that contributed to the results presented here.

References

Abouchami, W., Näthe, K., Kumar, A., Galer, S.J.G., Jochum, K.P., Williams, E., Horbe, A.M.C., Rosa, J.W.C., Balsam, W., Adams, D., Mezger, K., Andreae, M.O., 2013. Geochemical and isotope characterization of the Bodélé Depression dust source and implications for transatlantic dust transport to the Amazon Basin. Earth Planet. Sci. Lett. 380, 112–123.
Ammerman, J.S., Hood, R.R., Case, D.A., Cotner, J.B., 2003. Phosphorus deficiency in the Atlantic: an emerging paradigm on oceanography. Eos 84, 165.
Anderson, L.D., Faul, K.L., Paytan, A., 2010. Phosphorus associations in aerosols: what can they tell us about P bioavailability? Mar. Chem. 120, 44–56.
Atlas, E., Pytkowicz, R.M., 1977. Solubility behavior of apatites in seawater. Limnol. Oceanogr. 22, 290–300.
Baker, A.R., French, M., Linge, K.L., 2006a. Trends in aerosol nutrient solubility along a west–east transect of the Saharan dust plum. Geophys. Res. Lett. 33 L07805.
Baker, A.R., Jickells, T.D., Witt, M., Linge, K.L., 2006b. Trends in the solubility of iron, aluminium, manganese and phosphorus in aerosol collected over the Atlantic Ocean. Mar. Chem. 98, 43–58.
Barbarand, J., Cater, A., Wood, I., Hurford, T., 2003. Compositional and structural control of fission-track annealing in apatite. Chem. Geol. 198, 107–137.
Berner, R.A., Rao, J.-L., 1994. Phosphorus in sediments of the Amazon River and estuary: implications for the global flux of phosphorus to the sea. Geochim. Cosmochim. Acta 58, 2333–2339.
Boutinguiza, M., Pou, J., Comesaña, R., Lusquiños, F., de Carlos, A., León, B., 2012. Biological hydroxyapatite obtained from fish bones. Mater. Sci. Eng. C32, 478–486.
Bristow, C.S., Drake, N., Armitage, S., 2009. Deflation in the dustiest place on Earth: the Bodélé Depression, Chad. Geomorphology 105, 50–58.
Bristow, C.S., Hudson-Edwards, K.A., Chappell, A., 2010. Fertilizing the Amazon and equatorial Atlantic with West African dust. Geophys. Res. Lett. 37, L14807.
Chappell, A., Warren, A., O'Donoghue, A., Robinson, A., Thomas, A., Bristow, C.S., 2008. The implications for dust emission modeling of spatial and vertical variations in horizontal dust flux and particle size in the Bodélé Depression, northern Chad. J. Geophys. Res. 113, D04214.
Chen, H.-Y., Fang, T.-H., Preston, M.R., Lin, S., 2006. Characterization of phosphorus in the aerosol of a coastal atmosphere: using a sequential extraction method. Atmos. Environ. 40, 279–289.
Cooke, R., Jiménez, M., 2012. Pre-Columbian use of freshwater fish in the Santa Maria Biogeographical Province, Panama. Quat. Int. http://dx.doi.org/10.1016/j.quaint.2008.01.002.
Cury, J.A., Francisco, S.B., Simões, G.S., Del Bel Cury, A.A., Tabchoury, C.P.M., 2003. Effect of a calcium carbonate-based dentrifrice on enamel demineralization in situ. Caries Res. 37, 194–199.
Dolislager, L.J., VanCuren, R., Pederson, J.R., Lashgari, A., McCauley, E., 2012. A summary of the Lake Tahoe Atmospheric Deposition Study (LTADS). Atmos. Environ. 46, 618–630.
Drake, N., Bristow, C.S., 2006. Shorelines in the Sahara: geomorphological evidence for an enhanced monsoon from palaeolake Megachad. The Holocene 16, 901–911.
Eijsink, L.M., Krom, M.D., Herut, B., 2000. Speciation and burial flux of phosphorus in the surface sediments of the eastern Mediterranean. Am. J. Sci. 300, 483–504.
Filippelli, G.M., 2008. The global phosphorus cycle: past, present, and future. Elements 4, 89–95.
Förstner, U., Wittman, G.T.W., 1979. Metal Pollution in the Aquatic Environment, 1st ed. Springer-Verlag, New York.
Franke, R., Hormes, J., 1995. The P K-near edge absorption spectra of phosphates. Physica B 216, 85–95.
Fulmer, M.T., Ison, I.C., Hankermayer, C.R., Constantz, B.R., Ross, J., 2002. Measurements of the solubilities and dissolution rates of several hydroxyapatites. Biomaterials 23, 751–755.
Giguet-Covex, C., Poulenard, J., Chalmin, E., Arnaud, F., Rivard, C., Jenny, J.-P., Dorioz, J.-M., 2013. XANES spectroscopy as a tool to trace phosphorus transformation during soil

genesis and mountain ecosystem development from lake sediments. Geochim. Cosmochim. Acta 118, 129–147.
Ingall, E.D., Brandes, J.A., Diaz, J.M., de Jonge, M.D., Paterson, D., McNulty, I., Crawford Elliott, W., Northrup, P., 2011. Phosphorus K-edge XANES spectroscopy of mineral standards. J. Synchrotron Radiat. 18, 189–197.
Jahnke, R.A., 1992. The phosphorus cycle. In: Butcher, S.S., Charlson, R.J., Orians, G.H., Wolff, G.V. (Eds.), Global Geochemical Cycles. Academic Press, San Diego, pp. 301–315 (Chapter 14).
Khare, N., Hesterberg, D., Martin, J.D., 2005. XANES investigation of phosphate sorption in single and binary systems of iron and aluminum oxide minerals. Environ. Sci. Technol. 39, 2152–2160.
Kim, C.S., Brown, G.E., Rytuba, J.J., 2000. Characterization and speciation of mercury-bearing mine wastes using X-ray absorption spectroscopy. Sci. Total Environ. 261, 157–168.
Kohfeld, K.E., Tegen, I., 2007. Record of mineral aerosols and their role in the Earth system. Treatise on Geochemistry, 13, pp. 1–26 (Chapter 4).
Koren, I., Kaufman, Y.J., Washington, R., Todd, M.C., Rudich, Y., Martins, J.V., Rosenfeld, D., 2006. The Bodele depression: a single spot in the Sahara that provides most of the mineral dust to the Amazon forest. Environ. Res. Lett. 1, 014005.
Mackenzie, F.T., Ver, L.M., Sabine, C., Lane, M., Lerman, A., 1993. C, N, P, S global biogeochemical cycles and modeling of global change. In: Wollast, R., Mackenzie, F.T., Chou, L. (Eds.), Interactions of C, N, P and S Biogeochemical Cycles and Global Change. NATO ASI Series 1, vol. 4. Springer, Berlin, pp. 1–61.
Mahowald, N.M., Jickels, T.D., Baker, A.R., Artaxo, P., Benitez-Nelson, C.R., Bergametti, G., Bond, T.C., Chen, Y., Cohen, D.D., Herut, B., Kubilay, N., Losno, R., Luo, C., Maenhaut, W., McGee, K.A., Okin, G.S., Siefert, R.L., Tsukuda, S., 2008. Global distribution of atmospheric phosphorus sources, concentrations and deposition rates, and anthropogenic impacts. Global Biogeochem. Cycles 22, GB4026.
Mange, M.A., Maurer, H.F.W., 1991. Heavy Minerals in Colour. Chapman and Hall, London, UK.
Monbet, Ph., Brunskill, G.J., Zagorskis, I., Pfitzner, J., 2007. Phosphorus speciation in the sediment and mass balance for the central region of the Great Barrier Reef continental shelf (Australia). Geochim. Cosmochim. Acta 71, 2762–2779.
Nenes, A., Krom, M.D., Mihalopoulos, N., Van Cappellen, P., Shi, Z., Bougiatioti, A., Zarmpas, P., Herut, B., 2011. Atmospheric acidification of mineral aerosols: a source of bioavailable phosphorus for the oceans. Atmos. Chem. Phys. Discuss. 11, 6163–6185.
O'Donoghue, A.L., 2011. Mineral dust production in the Bodélé depression, Northern Chad. Unpublished PhD thesis, University of Salford, UK.
Okin, G., Mahowald, N., Chadwick, O., Artaxo, P., 2004. Impact of desert dust on the biogeochemistry of phosphorus in terrestrial ecosystems. Glob. Biogeochem. Cycles 18. http://dx.doi.org/10.1029/2003GB002145.
Pasteris, J.D., Wopenka, B., Valsami-Jones, E., 2008. Bone and tooth mineralization: why apatite? Elements 4, 97–104.
Pett-Ridge, J.C., 2009. Contributions of dust to phosphorus cycling in tropical forests of the Luqillo Mountains, Puerto Rico. Biogeochemistry 94, 63–80.
Ravel, B., 2009. ATHENA Users' Guide, version 1.5. http://cars9.uchicago.edu/~ravel/software/doc/Athena/html/athena.pdf.
Ravel, B., Newville, M., 2005. ATHENA, ARTEMIS, HEPHAESTUS: data analysis for X-ray absorption spectroscopy using IFEFFIT. J. Synchrotron Radiat. 12, 537–541.
Richey, J.E., 1983. The phosphorus cycle. In: Bolin, B., Cook, R.B. (Eds.), The Major Biogeochemical Cycles and Their Interactions. SCOPE, 21. Wiley, Chichester, pp. 51–56.
Ruttenberg, K.C., 2007. The global phosphorus cycle. Treatise on Geochemistry, 13, pp. 585–643 (Chapter 8).
Sanchez, P., Bandy, D., Villachica, J., Nicholaides, J., 1982. Amazon Basin soils: management for continuous crop production. Science 216, 812–827.
Schepanski, K., Tegen, I., Macke, A., 2009. Saharan dust transport and deposition towards the tropical northern Atlantic. Atmos. Chem. Phys. 9, 1173–1189.
Schuster, M., Roquin, C., Duringer, P., Brunet, M., Caugy, M., Fontugne, M., Mackaye, H.T., Vignaud, P., Ghienne, J.-F., 2005. Holocene lake Mega-Chad palaeoshorelines from space. Quat. Sci. Rev. 24, 1821–1827.
Schuster, M., Duringer, P., Ghienne, J.-F., Roquin, C., Sepulchre, P., Moussa, A., Lebatard, A.-E., Mackaye, H.T., Likius, A., Vignaud, P., Brunet, M., 2009. Chad Basin: palaeoenvironments of the Sahara since the Late Miocene. Compt. Rendus Geosci. 341, 603–611.
Schwertmann, U., Cornell, R.M., 1991. Iron Oxides in the Laboratory: Preparation and Characterisation. VCH Publishers, New York, USA.
Singer, A., Dultz, S., Argaman, E., 2004. Properties of the nonsoluble fractions of suspended dust of the Dead Sea. Atmos. Environ. 38, 1745–1753.
Smits, M.M., Bonneville, S., Benning, L.G., Banwart, S.A., Leake, J.R., 2012. Plant-driven weathering of apatite — the role of an ectomycorrhizal fungus. Geobiology 10, 445–456.
Swap, R., Garstang, M., Greco, S., Talbot, R., Kallberg, P., 1992. Saharan dust in the Amazon Basin. Tellus Ser. B 44, 133–149.
Tenderholt, A., Hedman, B., Hodgson, K.O., 2007. PySpline: a modern, cross-platform program for the processing of raw averaged XAS edge and EXAFS data. AIP Conf. Proc. (XAFS13), 882, pp. 105–107.
Washington, R., Todd, M.C., 2005. Atmospheric controls on mineral dust emission from the Bodele Depression, Chad: the role of the Low Level Jet. Geophys. Res. Lett. 32 (Art. No. L17701).
Washington, R., Todd, M.C., Middleton, N., Goudie, A.S., 2003. Dust-storm source areas determined by the total ozone monitoring spectrometer and surface observations. Ann. Assoc. Am. Geogr. 93, 297–313.
Washington, R., Todd, M., Engelstaedter, S., Mbainayel, S., Mitchell, F., 2006. Dust and the low-level circulation over the Bodélé Depression, Chad: observations from BoDEx 2005. J. Geophys. Res. 111, DO3201.
Winter, J.G., Dillon, P.J., Futter, M.N., Nicholls, K.H., Scheider, W.A., Scott, L.D., 2002. Total phosphorus budgets and nitrogen loads: Lake Simcoe, Ontario (1990 to 1998). J. Great Lakes Res. 28, 301–314.